

Impinging Cooling with a Crescent Surface Inspired by Barchan Dunes in a Simplified Gas Turbine Transition Section

GUO Haotian¹, XU Tao¹, LIANG Xiao¹, YU Zhenglei^{2*}, XING Genyuan¹,
GUO Huan³

1. College of Mechanical Science and Aerospace Engineering, Jilin University, Changchun 130022, P. R. China;

2. Key Lab of Bionic Engineering, Ministry of Education, Jilin University, Changchun 130022, P. R. China;

3. Aviation University of Air Force, Changchun 130022, P. R. China

(Received 20 March 2019; revised 22 June 2019; accepted 25 September 2019)

Abstract: For the enhancement of heat transfer efficiency, a novel turbulator inspired by the morphology of barchan dunes, called the mimetic barchan dune (MBD) turbulator, is designed and evaluated in the simplified gas turbine transition section. By using computational fluid dynamics (CFD), the numerical simulations for comparison have been carried out, concluding the smooth thermal surface, a thermal surface with riblet-shaped turbulator and a thermal surface with MBD turbulator. Then, two indicators are investigated for evaluating the coolant performance which are the heat transfer efficiency (η) on the outlet and the pressure loss (ΔP) in the coolant chamber. The numerical results show that the coolant has the best heat transfer efficiency with less pressure loss in the coolant chamber with the MBD turbulator. Then, the effect of the MBD turbulator sizes on heat transfer efficiency is investigated. When the height of the MBD turbulator (h) is set at 8 mm, the maximum amount of heat that could be transferred by the coolant is up to 566.2 K and the corresponding heat transfer efficiency is 26.62%. The detail flows have been shown to elucidate the function of the MBD surface which may greatly arouse more design for solving harsh circumstance.

Key words: convective heat transfer; gas turbine; simplified transition piece model; mimetic thermal surface; barchan dunes; computational fluid dynamics (CFD)

CLC number: TB17

Document code: A

Article ID: 1005-1120(2019)05-0760-09

0 Introduction

Effective heat exchangers are key components of heat engines to ensure the efficient use of energy due to the lack of the non-renew energy resources. Currently, gas turbine is a popular device for power conversion which design is limited by the heat resistance of the transition section^[1]. The increasing turbine entry temperature is one of the ways for improving the cycle thermodynamic efficiency for a given cycle under the optimum pressure ratio^[2]. However, high gas turbine entry temperature will threaten the working lifespan and the reliability of the transition section, and even melt the turbine material^[3]. In order to provide a new design or to improve the

performance of a gas turbine, it is a necessary premise that thermal protection for the transition section is investigated.

The transition section, transporting the combustion gases between the combustor and turbine, has been studied for its cooling. Munoz et al.^[4] considered that different dimensions of the transition section designed by a genetic algorithm affected the gas temperature and velocity in the outlet area. By using computational fluid dynamics (CFD), the gas temperature and velocity profiles in the transition section were presented. Then, a geometry optimization of the transition section was estimated. The new design of the transition section reduced the av-

*Corresponding author, E-mail address: yuzhenglei@hotmail.com.

How to cite this article: GUO Haotian, XU Tao, LIANG Xiao, et al. Impinging Cooling with a Crescent Surface Inspired by Barchan Dunes in a Simplified Gas Turbine Transition Section[J]. Transactions of Nanjing University of Aeronautics and Astronautics, 2019, 36(5): 760-768.

<http://dx.doi.org/10.16356/j.1005-1120.2019.05.007>

erage turbine inlet temperature by about 2.32% and the average velocity by about 7.73%.

A sheath with regular-arranged holes, which was wrapping the transition section and combustor, was tested by Wang et al.^[5-6] for cooling the thermal surface. They employed both experimental and computational methods to confirm the value of the sheath. The case without the sheath had a 40% reduction in the pressure loss compared with the case adding the sheath. However, a 35% increase in the maximum surface temperature difference and an increase of 13%—22% in other surface temperature difference, based on the temperature difference of the bulk inlet and outlet temperature. Wang et al. concluded that removing of the sheath was not recommended unless a better cooling method could replace it.

Yu and Xu et al.^[7] investigated the effects of the coolant orientation and the impinging hole's angles on the heat transfer efficiency in a simplified transition section designed as a one-fourth cylinder. A series of CFD numerical simulations showed that the heat transfer efficiency was the best when both the hole inclination and the injection angle are 90°. They mixed droplets into the coolant for heat transfer^[8]. Comparison of different diameters and mass of the droplet were investigated, and the results showed that the performance of the coolant flows were the best, when the mass flow rate of the droplets was 3×10^{-3} kg/s and the diameters were from 5 μm to 35 μm .

The above-mentioned works are focused on the smooth wall heat transfer target in the process of impingement cooling. In fact, it is also a good way to strengthen the hot-section heat protection that a new structural design on the thermal surface is used as the impact target surface in the gas turbine transition section. For improving the performance of the coolant flow, a thermal surface with pin fins was studied^[9]. They concluded that the cooling efficiency was increased without excessive pressure loss, when the pin fins were brought in. The optimal size of pin fins and the mass of the mist made the value of the average temperature reduced by 42.65 K in the coolant chamber.

In addition to adding pin fins in the cooling chamber, other designs have been tested to enhance the thermal protection of the impinging cooling, such as ribs^[10-13] and protrusions^[14-16]. However, it is difficult to find out the best solution between enhancing the formation of turbulence and reducing the pressure loss. In other words, it is a huge challenge to design a thermal surface for heat engineers.

Nowadays, many excellent structures and morphologies in nature have provided a lot of inspirations to engineers. Some analysis indicated that the non-smooth surface of organisms evolved to alter the surrounding flow characteristics to better satisfy their own needs. Cui and Fu^[17] designed four kinds of the biomimetic groove surfaces with nano-structural units, which were inspired by sharks, jaegers, seals and shells. Then, Cui and Fu^[17] used the lattice Boltzmann method (LBM) to understand how the biomimetic surface reduced drag. Cui and Fu^[17] concluded that the riblet-shaped structure inspired by skin of seals had the lowest flow resistance and the ridge-shaped one inspired by outside surface of shells had the lowest drag reduction in on mesoscopic level.

Bajanski et al.^[18] examined a windbreak fence inspired by the shark skin denticle geometry to slow down the wind in open and urban areas. The difference of air velocity distribution between the biomimetic and a benchmark smooth windbreak fence was studied by CFD. The biomimetic design was found to be attractive.

Zhou and co-workers^[19-21] analyzed the film cooling efficiency of the coolant, which jetting under a sand-dune-inspired surface. During the experiments, the sand-dune-inspired surface made the coolant flow attach to the target surface more firmly, which was used as additional coolant inlet coat. These results showed that the new design worked very well for the increasing of the cooling efficiency. However, the pressure loss performance was not optimistic, when the coolant was blown in at a low speed ratio.

This study indicates that the flow characteristics around the structures and morphologies in nature can be used to provide the hot-section thermal

protection to the transition section of a gas turbine. In this paper, inspired by the morphology of the barchan dunes, a simplified double-chamber model with mimetic barchan dune (MBD) turbulators is designed and investigated for enhancing heat transfer efficiency. The MBD turbulators on the heat transfer surface will enhance the impinging cooling efficiency with little pressure loss by changing the coolant flow characteristics. To compare the flow characteristics in the simplified transition section with different thermal surfaces, numerical simulations were performed. The simulations provided predictions of the flow streamline in the coolant chamber. It also provided predictions for the average temperature and the pressure loss on the coolant outlet facets, which had been turn out to be a cost-effective approach.

1 Concept Generators and Mimetic Design

The barchan dune, which is commonly seen in deserts, is generated by an uni-directional wind flow^[22]. Its surface can be described as a crescentic platform and a streamline shape along the flow direction, as shown in Fig.1^[23-24]. The stream shape has the windward side and leeward side along with two gradually-narrowed tails pointing downstream. When it is blown by the air with sand particles, the shape of a dune will become a crescent platform of streamline cross section by dynamic stability^[25]. Therefore, it can be inferred that less shear force will be generated on the new concept thermal surface and a pair of coolant vortices will be formed by

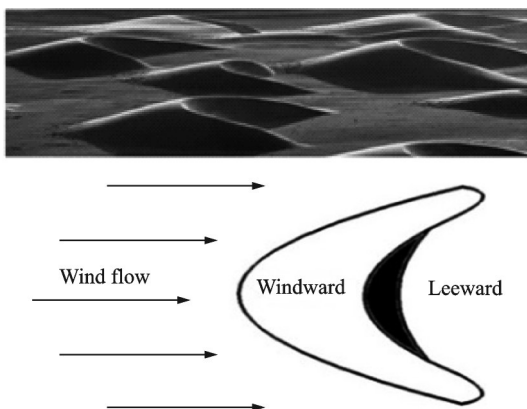


Fig.1 Morphology of barchan dunes

the guidance of the two gradual narrowed tails, as the coolant flows along the streamline-shape barchan surface. It is expected that turbulators with the shape of barchan dunes can enhance the heat transfer efficiency of impinging cooling at a lower pressure loss across the coolant chamber. In order to verify the validity of the above ideas, numerical simulations are carried out by using CFD on the simplified transition section with a biomimetic barchan dune model shown in Fig.2(a). The height of the MBD turbulator is h , and the width is $6h$. The other dimensions of the MBD turbulator are shown in Fig.2(b). $L = 5h$ is the length of the dune along the direction of the coolant flow. $l_1 = 1.5h$ and $l_2 = h$ are the horizontal distances from the top to the front and from the top to the behind of the MBD turbulator in the mid-span symmetry plane, respectively. In the gas turbine transition piece, the MBD turbulator is located at the horizontal distance of 40 mm from the coolant hole along the flow direction.

Fig.3 shows the structure of the transition section in the gas turbine. The flow of the coolant and the mainstream are both signed to express the cooling theory. There are hundreds of cooling holes on the top sheat. In this paper, a double-channel box-shaped computational domain is defined. This represents a simplified gas turbine transition piece by eliminating the influence by curvature on impinging cooling. Fig.2(a) shows the overall dimensions of the double-channel domain. The height of coolant chamber and gas chamber are 38 mm and 162 mm, respectively. The length and the width of the prismatic computational domain are set as 1 050 mm and 320 mm, respectively. The bottom boundary surface of the domain and the side walls are modelled as the symmetric flow boundaries. In the top of the coolant chamber, there are three holes for jetting the coolant, as displayed in Fig.2(a). The diameter ϕ of the coolant inlet holes is set at 10 mm and the space between them is 106.67 mm. In Section 1, h is set as 5 mm in the simplified transition piece with the MBD turbulators. In order to study the effect of the turbulators' morphology on coolant flow characteristics, a riblet-shaped turbulator as benchmark is chosen to compare with the MBD tur-

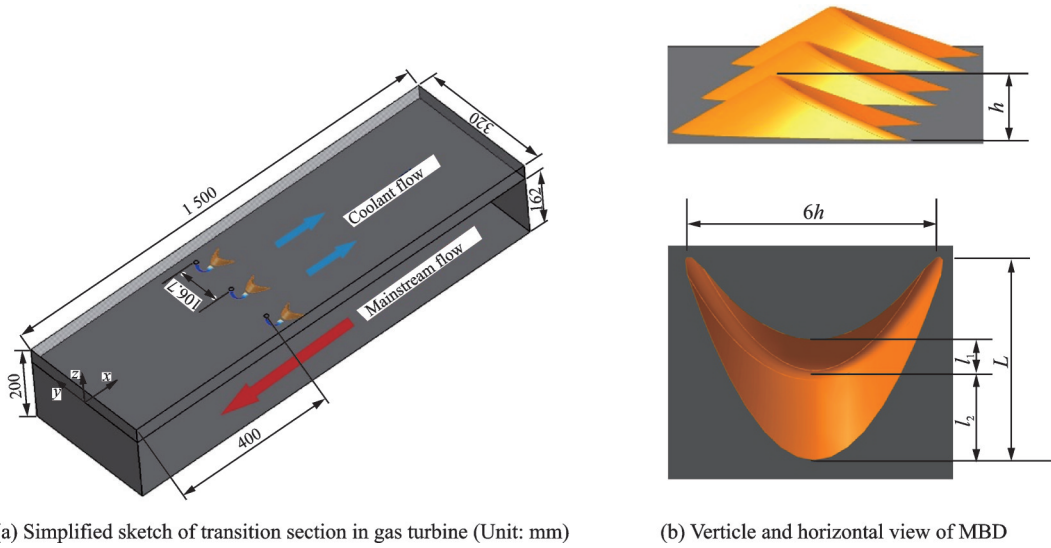


Fig.2 Simplified sketch of transition piece with MBD turbulators

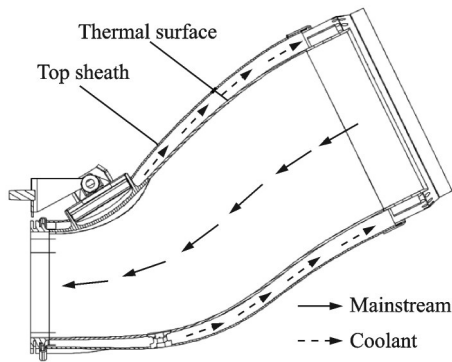


Fig.3 Structure of transition section

turbulator. The calculation domain with rib is the same as that with dune. The height and width of the riblet-shaped turbulator are 5 mm and 7.5 mm, respectively, as shown in Fig.4. In Section 2, h is varied from 5 mm to 17 mm, and the step is 1.5 mm. In order to infer trends of the heat transfer efficiency, 9 different sizes of the MBD turbulators are considered.

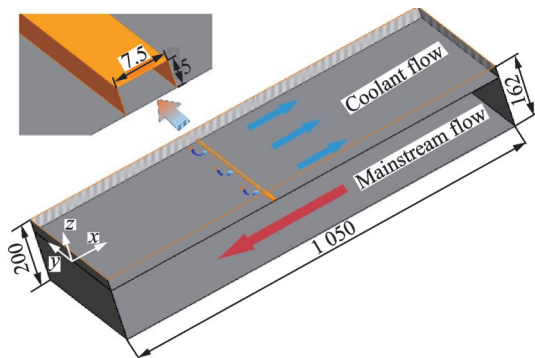


Fig.4 Riblet-shaped turbulators

2 Working Condition and Evaluation Function

According to the predecessor's confirmation^[7], it is chosen in this study that coolant hole angle and injection orientations are orthogonal to the thermal surface. During one F-class gas turbine operation, the gas transported from the combust has the temperature of 1 300 K and the mass flow rate of 32.72 kg/s. In the coolant chamber, pressure inlet chosen as jet holes' initial conditions is set as 1.822 MPa, and the temperature of the coolant is 300 K. Details of the boundary conditions are given in Table 1^[26]. In the mainstream chamber, it is assumed that the mainstream is a mixture of N_2 , O_2 , H_2O , SO_2 and CO_2 , as well as rare gases. Their

Table 1 Boundary conditions^[26]

Component	Boundary condition	Magnitude
Mainstream inlet	Mass flux rate/($kg \cdot s^{-1}$)	32.72
	Gas temperature/K	1 300
	Turbulent intensity/%	5
	Hydraulic diameter/m	0.324
Mainstream outlet	Pressure/MPa	1.573
	Turbulent intensity/%	5
	Hydraulic diameter/m	0.324
Coolant chamber	Air temperature/K	300
	Pressure/MPa	1.822
	Pressure recovery coefficient	0.95
	Turbulent intensity/%	10
	Hydraulic diameter/m	0.010

volume fractions are 0.729 471 1, 0.087 987 4, 0.067 862 8, 0.000 214 2 and 0.114 464 5, respectively. In another chamber, air as the coolant is used for all of the simulations. The material of the thermal surface uses Nimonic 263 (the density is 8 360 kg/m³, the specific heat is 569 J/(kg•K), the thermal conductivity is 30.16 W/(m•K)), for which information could be found from internet. The thickness of the thermal surface is 6.8 mm.

The flows in these simplified calculated models are steady, Newtonian, three-dimensional, incompressible, turbulent, and behave according to three fundamental laws: continuity, and the conservation of momentum and energy. The realizable k - ϵ turbulence model with the enhanced wall function is chosen to simulate the flow behaviors and the convective heat transfer enhancement on the biomimetic thermal surface^[7]. All of the runs were solved on a workstation with an eight cores i7 3.6 GHz CPU. The decreasing of the energy residual by 10^{-6} is chosen to be the standard of convergence tolerance during 5 000 solving iterations.

In order to determine the quantity of heat that is taken away in the process of heat exchange in the coolant chamber, the average temperature based on mass flow rate λ , which is provided as an indicator that is computed by the product of flow rate and temperature, and it is defined as

$$\lambda = \int T \rho \mathbf{v} \cdot d\mathbf{A} = \sum_{i=1}^n T_i \rho_i \mathbf{v}_i \cdot \mathbf{A}_i \quad (1)$$

where ρ is the density of the coolant and \mathbf{v} the facet velocity on the selected field. The mass flow rate can be defined as

$$R_{\text{massflow}} = \int \rho \mathbf{v} \cdot d\mathbf{A} = \sum_{i=1}^n \rho_i \mathbf{v}_i \cdot \mathbf{A}_i \quad (2)$$

According to Eqs. (1) and (2), the average temperature based on mass flow rate can be described as follows on the coolant outlet surface

$$T_{\text{ave}} = \frac{\lambda}{R_{\text{massflow}}} = \frac{\sum_{i=1}^n T_i \rho_i \mathbf{v}_i \cdot \mathbf{A}_i}{\sum_{i=1}^n \rho_i \mathbf{v}_i \cdot \mathbf{A}_i} \quad (3)$$

And the heat transfer efficiency can be defined as

$$\eta = \frac{T_{\text{ave}} - T_{\text{inlet}}}{T_c} \quad (4)$$

which serves as an indicator to value the perfor-

mance of impinging cooling. In Eq. (4), T_{inlet} is set as 300 K, and T_c is defined as

$$T_c = T_{\text{gas}} - T_{\text{inlet}} \quad (5)$$

where T_{gas} represents for the gas temperature.

Finally, the pressure loss can be computed as

$$\Delta P = P_{\text{in}} - P_{\text{out}} \quad (6)$$

where P_{in} is the pressure on the coolant holes, and P_{out} the total pressure on the outlet.

3 Results and Discussion

3.1 Comparison of grid sensitivity

The simplified model, consisting of tetrahedral meshes, is solved in the software ANSYS-ICEM, version 18.2. In order to acquire accurate results, a grid sensitivity study is performed in the double-chamber transition piece, which is made up by the smallest size ($h = 5$ mm) of the MBD turbulator. Increasing the mesh spatial resolution will improve the accuracy of the numerical solution, but the time for calculation will also increase with it. Therefore, the appropriate mesh size should be identified so that the calculation can be completed quickly and accurately. In Table 2, the number of mesh is 0.17, 0.48, and 0.7 million, respectively. When the number increases to 0.7 million, the average temperature on the coolant outlet is 548.34 K, only increasing about 1 K than the temperature when the mesh number is 0.48 million. The deviation is less than 0.2%, so it is considered that the result is correct when the mesh number is more than 0.48 million.

Table 2 Test for grid sensitivity

Mesh number/million	T_{ave}/K
0.17	539.30
0.48	547.39
0.70	548.34

3.2 Comparison of performance of different thermal surfaces

For investigating the effect of turbulator and its morphology on the impinging coolant flow, three cases are designed, which are the simplified transition piece model with a smooth thermal surface, a

riblet-shaped thermal surface and a MBD surface, respectively. The average temperature and the pressure loss are calculated as valuating indicators, whose averaged method are based on the mass flow rate of the outlet surface in Fig.5.

Fig.5 shows that the coolant chambers with different thermal surfaces can reduce the coolant outlet flow temperature to about 536.45, 544.27 and 547.39 K, respectively. Meanwhile the pressure loss through the transition duct is 198 306.14, 198 518.07 and 198 438.90 Pa, respectively. It is concluded that the simplified transition piece model with the non-smooth thermal surface both can carry off more heat than the model with the smooth thermal surface from the coolant chamber, at a higher-pressure loss. In Fig.5, it is confirmed that the performance of the MBD model is better than the riblet-shaped surface in the coolant chamber since more heat is forced to take out at less pressure loss.

Fig.6 shows the temperature contours and flow

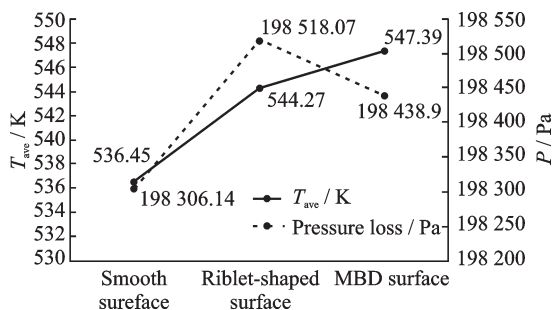


Fig.5 Temperature on the outlet and pressure loss

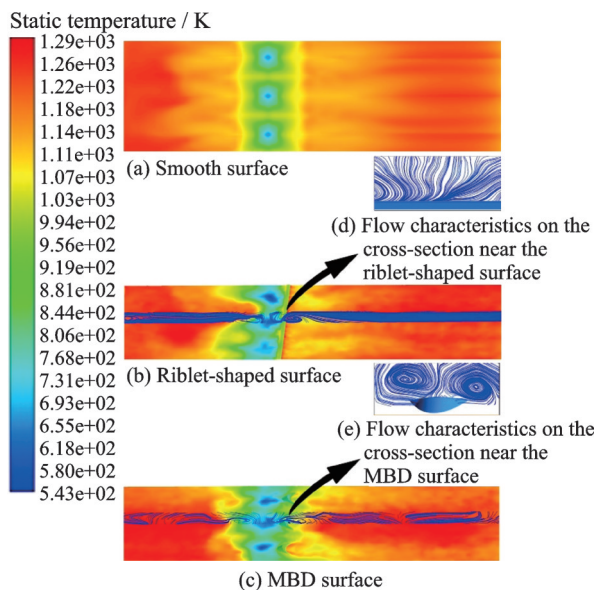


Fig.6 Comparison of flow characteristics and temperature distribution on the thermal surface

characteristics on the thermal surfaces, which are the smooth surface and the non-smooth surfaces. Figs.6(a—c) suggest that small cold spots form below the impacting jets on the smooth thermal surface, but cold spots of larger area form on the non-smooth surfaces. For studying the function of the turbulators, streamlines along the coolant flow direction are depicted in Figs.6(b, c). Meanwhile, Figs.6(d, e) show sections parallel with the YZ plane with streamlines of in-plane velocity. Fig.6(b) shows that a vortex is generated behind the riblet-shaped turbulator above the thermal surface, by the coolant flow over the rectangular rib. However, it can be seen in Fig.6(c) that the coolant flows along the streamline shape windward slope and a reverse flow is formed for the reduction of heat accumulation behind the turbulators on the thermal surface. In fact, it can be deduced that the flow vector is mainly altered by the ribbed turbulator in the two-dimensional space and the change of the coolant vector is more complicated with the crescent dune turbulators. In Fig.6(d), the coolant in-plane streamlines do not form Y -wise vortices. However, after the coolant flows through streamlined upwind slopes, a pair of Y -wise vortices, which are symmetric nearby the dune tails, are formed for changing the convective heat transfer efficiency in Fig.6(e). These vortices affect the surface temperature distribution. Therefore, the design of the MBD turbulator promotes generation of vortices and thereby improve the convective heat transfer efficiency.

3.3 Comparison of different sizes of MBD turbulator

In this section, the effect of the sizes of the MBD turbulator on heat transfer efficiency is investigated by varying the height h . h is set from 5 mm to 17 mm, in 1.5 mm increments. The average temperature on the coolant outlet and the heat transfer efficiency are both calculated according to Eqs.(1—5) and are shown in Table 3. In Fig.7, it is shown that $h = 8$ mm delivers the best heat transfer efficiency which is 26.62% and $h = 5$ mm has the worst. However, it is only 1.88% below that of $h = 8$ mm. That is, the range of the performance is small

Table 3 Average temperature and heat transfer efficiency in Section 2

n	h/mm	T_{ave}/K	$\eta/\%$
1	5	547.4	24.74
2	6.5	557.4	25.74
3	8	566.2	26.62
4	9.5	561.9	26.19
5	11	560.5	26.05
6	12.5	558.0	25.80
7	14	556.7	25.67
8	15.5	552.3	25.23
9	17	550.6	25.06

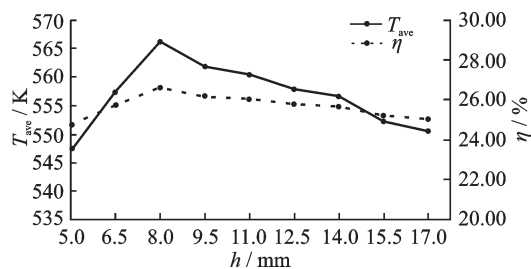


Fig.7 Average temperature and heat transfer efficiency in Section 2

among all h . Although the absolute difference between the best and the worst performance is small among all h , some slight trends can be found out. Over the range $5 \text{ mm} \leq h \leq 8 \text{ mm}$, the average temperature increases with the size increase of the MBD turbulator on the coolant outlet. Over the range $8 \text{ mm} \leq h \leq 17 \text{ mm}$, the average temperature as well as the heat transfer efficiency reduce.

Based on CFD Fluent software, version 18.2, it is confirmed that the vortices shown as Fig.6(e) expand and interact more with each other gradually when h increases from 5 mm to 8 mm. In the comparison of varieties of different MBD turbulator dimensions, the space of the vortex becomes narrow nearby the dune tails as the size increases. The convective heat transfer performance is influenced by changes in the vortices on the thermal surface. It seems to be the main reason driving the changes in the heat transfer efficiency with the sizes of the MBD turbulator.

4 Conclusions

The MBD shaped turbulator inspired by the barchan dunes is designed in a simplified gas turbine

transition section. In order to understand peculiar of the MBD turbulators, the comparison of different thermal surfaces is performed, which includes the smooth thermal surface, the riblet-shaped thermal surface, and the MBD thermal surface. After adding the turbulator devices, the heat transfer efficiency of the impinging cooling is elevated in the coolant chamber. However, more pressure loss is also brought in with the non-smooth surface. Compared with the riblet-shaped surface, the idealized transition piece model with the MBD turbulator has a higher convective heat transfer efficiency with less pressure loss.

Then, the effect of the MBD size on the heat transfer efficiency is investigated. When h is set as 8 mm, the maximum amount of heat that can be taken away by the coolant is up to 566.2 K and the corresponding heat transfer efficiency is 26.62%. When $h < 8 \text{ mm}$, the average outflow temperature increases with the size h of the MBD turbulator on the coolant outlet; when $h > 8 \text{ mm}$, this trend reverses. However, the range of flow temperature and cooling efficiency obtained by varying the MBD size is relatively small.

The above conclusion provided that the design of the MBD turbulator is significant in the application of forced convective heat exchange enhancement, which has a crescent platform and a complex streamline surface consisted of upward and leeward slopes. The design and research on the crescent turbulator may offer a new sight of the impingement cooling efficiency, especially for the heat protection, which confront a similar severe working condition.

References

- [1] DA SOGHE R, BIANCHINI C, ANDREINI A, et al. Thermofluid dynamic analysis of a gas turbine transition-Piece [EB/OL]. [2015-01-01]. <https://doi.org/10.1115/1.4028869>.
- [2] GAD-BRIGGS A, PILIDIS P, NIKOLAIDIS T. A review of the turbine cooling fraction for very high turbine entry temperature helium gas turbine cycles for generation IV reactor power plants[EB/OL]. [2017-03-01]. <https://doi.org/10.1115/1.4035332>.
- [3] XUE R, HU C, SETHI V, et al. Effect of steam ad-

- dition on gas turbine combustor design and performance[J]. *Applied Thermal Engineering*, 2016, 104: 249-257.
- [4] MUNOZ A G, AYALA-RAMIREZ V, ALFARO-AYALA J A, et al. Optimization of the transition piece applying genetic algorithms[J]. *Applied Thermal Engineering*, 2011, 31(16): 3214-3225.
- [5] WANG L, WANG T. Investigation of the effect of perforated sheath on thermal-flow characteristics over a gas turbine reverse-flow combustor, Part 1—Experiment[C]//*Proceedings of the ASME Turbo Expo: Turbine Technical Conference and Exposition*. San Antonio, TX: ASME, 2013.
- [6] WANG L, WANG T. Investigation of the effect of perforated sheath on thermal-flow characteristics over a gas turbine reverse-flow combustor, Part 2—Computational analysis[C]//*Proceedings of the ASME Turbo Expo: Turbine Technical Conference and Exposition*. San Antonio, TX: ASME, 2013.
- [7] YU Z L, XU T, LI J L, et al. Comparison of a series of double chamber model with various hole angles for enhancing cooling effectiveness[J]. *International Communications in Heat and Mass Transfer*, 2013, 44: 38-44.
- [8] YU Z L, XU T, LI J L, et al. Computational analysis of Droplet mass and size effect on mist/air impingement cooling performance [EB/OL]. [2015-01-26]. <https://doi.org/10.1155/2013/181856>.
- [9] XU T, XIU H, LI J L, et al. Simulation of impinging cooling performance with pin fins and mist cooling adopted in a simplified gas turbine transition piece [EB/OL]. [2014-03-09]. <http://dx.doi.org/10.1155/2014/327590>.
- [10] GUO H T, LIANG X, YU Z L, et al. Heat transfer designed for bionic surfaces with rib turbulators inspired by Alopias Branchial arch in a simplified gas turbine transition piece [EB/OL]. [2018-05-19]. <https://doi.org/10.3390/app8050820>.
- [11] JIANG G W, SHI X J, CHEN G W, et al. Study on flow and heat transfer characteristics of the mist/steam two-phase flow in rectangular channels with 60 Deg. ribs[J]. *International Journal of Heat and Mass Transfer*, 2018, 120: 1101-1117.
- [12] SINGH P, LI W H, EKKAD S V, et al. Experimental and numerical investigation of heat transfer inside two-pass rib roughened duct (AR=1:2) under rotating and stationary conditions[J]. *International Journal of Heat and Mass Transfer*, 2017, 113: 384-398.
- [13] YANG Y T, TANG H W, WONG C J. Numerical simulation and optimization of turbulent fluids in a three-dimensional angled ribbed channel[J]. *Numerical Heat Transfer Part A—Applications*, 2016, 70(5): 532-545.
- [14] SUN H O, SUN T, YANG L F, et al. Effect of bleed hole on internal flow and heat transfer in matrix cooling channel[J]. *Applied Thermal Engineering*, 2018, 136: 419-430.
- [15] SHEN Z Y, QU H C, ZHANG D, et al. Effect of bleed hole on flow and heat transfer performance of U-shaped channel with dimple structure[J]. *International Journal of Heat and Mass Transfer*, 2013, 66: 10-22.
- [16] XIE G N, SUNDEN B, ZHANG W H. Comparisons of pins/dimples/protrusions cooling concepts for a turbine blade tip-wall at high Reynolds numbers [EB/OL]. [2011-03-10]. <https://doi.org/10.1115/1.4003558>.
- [17] CUI J, FU Y B. A numerical study on pressure drop in microchannel flow with different bionic micro-grooved surfaces[J]. *Journal of Bionic Engineering*, 2012, 9(1): 99-109.
- [18] BAJANSKI I, STOJAKOVIC V, TEPAVCEVIC B, et al. An application of the shark skin denticle geometry for windbreak fence design and fabrication[J]. *Journal of Bionic Engineering*, 2017, 14(3): 579-587.
- [19] ZHOU W W, HU H. A novel sand-dune-inspired design for improved film cooling performance[J]. *International Journal of Heat and Mass Transfer*, 2017, 110: 908-920.
- [20] ZHOU W W, PENG D, WEN X, et al. Unsteady analysis of adiabatic film cooling effectiveness behind circular, shaped, and sand-dune-inspired film cooling holes: Measurement using fast-response pressure-sensitive paint[J]. *International Journal of Heat and Mass Transfer*, 2018, 125: 1003-1016.
- [21] ZHOU W W, HU H. Improvements of film cooling effectiveness by using barchan dune shaped ramps[J]. *International Journal of Heat and Mass Transfer*, 2016, 103: 443-456.
- [22] GREELEY R, BRIDGES N T, KUZMIN R O, et al. Terrestrial analogs to wind-related features at the viking and pathfinder landing sites on mars [EB/OL]. [2002-01-31]. <https://doi.org/10.1029/2000JE001481>.
- [23] HERSEN P. On the crescentic shape of barchan dunes[J]. *European Physical Journal B*, 2004, 37(4): 507-514.
- [24] HERSEN P. Flow effects on the morphology and dynamics of aeolian and subaqueous barchan dunes [EB/

- OL]. [2005-11-16]. <https://doi.org/10.1029/2004JF000185>.
- [25] HERSEN P, ANDERSEN K H, ELBELRHITI H, et al. Corridors of barchan dunes: Stability and size selection[EB/OL]. [2004-01-29]. <https://doi.org/10.1103/PhysRevE.69.011304>.
- [26] ARTURO A A J, ARMANDO G M, MANUEL R A J, et al. Analysis of the flow in the combustor-transition piece considering the variation in the fuel composition[C]//Proceedings of the ASME International Heat Transfer Conference. Washington, DC:ASME, 2010, 3: 245-257.

Acknowledgements The work was supported by the National Key R&D Program of China (No.2018YFB1105100), the National Natural Science Foundation of China (No.51975246), the Advanced Manufacturing Project of Provincial School Construction of Jilin Province (No. SXGJSF2017-2), the Program for JLU Science and Technology Innovative Research Team (2019TD-34), and the China Postdoctoral Science Foundation Funded Project (No. 2016M590256).

Authors Mr. GUO Haotian received the B.S. degree from Northeast Forest University in 2012 and the M.S. degree from Jilin University in 2016, respectively. Now he is a Ph.D. candidate of School of Mechanical and Aerospace Engineering, Jilin University.

Prof. XU Tao received the B.S. degree in computational mathematics from Jilin University in 1982 and the Ph.D. degree from Jilin University in 1996, respectively. Now she is a professor in School of Mechanical and Aerospace Engineer-

ing, Jilin University.

Mr. LIANG Xiao received the B.S. degree from Changchun University of Technology in 2015 and the M.S. degree from Jilin University in 2018, respectively. Now he is a Ph.D. candidate of School of Mechanical and Aerospace Engineering, Jilin University.

Prof. YU Zhenglei received the B.S. degree from Changchun University of Science and Technology in 2007 and the M.S. degree from Jilin University in 2011, respectively. He received his Ph.D. degree from Jilin University in 2014. Now he is a professor in School of Mechanical and Aerospace Engineering in Jilin University, Changchun, China.

Mr. XING Genyuan received the B.S. degree from Nanchang University in 2016. Now he is a postgraduate of School of Mechanical and Aerospace Engineering, Jilin University.

Ms. GUO Huan received the B.S. degree from Northeast Normal University in 2006 and the M.S. degree from Jilin University in 2008, respectively. In 2009, she joined Aviation University of Air Force, Changchun, China.

Author contributions Mr. GUO Haotian designed the study, conducted the analysis and wrote the manuscript. Mr. LIANG Xiao contributed to data for the analysis of average temperature and flow characteristics. Prof. XU Tao and Prof. YU Zhenglei contributed to the discussion and background of the study. Mr. XING Genyuan and Ms. GUO Huan contributed to finish the numerical tests.

Competing interests The authors declare no competing interests.

(Production Editor: Xu Chengting)